

The wave state and sea spray related parameterization of wind stress applicable from low to extreme winds

Bin Liu,^{1,2} Changlong Guan,¹ and Lian Xie²

Received 28 November 2011; revised 21 May 2012; accepted 23 May 2012; published 3 July 2012.

[1] Recent field and laboratory observations indicate that the variation of drag coefficient with wind speed at high winds is different from that under low-to-moderate winds. By taking the effects of wave development and sea spray into account, a parameterization of sea surface aerodynamic roughness applicable from low to extreme winds is proposed. The corresponding relationship between drag coefficient and sea surface wind speed agrees well with the existing field and laboratory observational data. It is shown that, under low-to-moderate wind conditions so that the sea spray effects could be neglected, the nondimensional aerodynamic roughness first increases and then decreases with the increasing wave age; whereas under high wind conditions, the drag coefficient decreases with the increasing wind speed due to the modification of the logarithmic wind profile by the effect of sea spray droplets produced by bursting bubbles or wind tearing breaking wave crests. The drag coefficients and sea surface aerodynamic roughnesses reach their maximum values when the 10 m wind speeds are between 25 and 33 m s⁻¹ for different wave developments. Correspondingly, the reduction of drag coefficient under high winds reduces the increasing rate of friction velocity with increasing wind speed.

Citation: Liu, B., C. Guan, and L. Xie (2012), The wave state and sea spray related parameterization of wind stress applicable from low to extreme winds, *J. Geophys. Res.*, 117, C00J22, doi:10.1029/2011JC007786.

1. Introduction

[2] Sea surface wind stress is the primary driving force for ocean currents and surface waves. Parameterization of wind stress over the air-sea interface is essential to many aspects of air-sea interaction, which in turn is vital for atmospheric, oceanic and surface wave prediction models, as well as climate modeling. During the past several decades, lots of studies based on laboratory and field observations and/or theoretical analyses [e.g., Charnock, 1955; Stewart, 1974; Wu, 1980; Geernaert et al., 1987; Donelan, 1990; Toba et al., 1990; Smith et al., 1992; Yelland and Taylor, 1996; Johnson et al., 1998; Drennan et al., 2003; Lange et al., 2004; Gao et al., 2006; Edson et al., 2007; Petersen and Renfrew, 2009] were conducted to determine sea surface wind stress through parameterization of drag coefficient or aerodynamic roughness.

[3] The air-sea momentum flux, i.e., wind stress τ can be estimated through the bulk aerodynamic method in terms of drag coefficient C_d

$$\tau \equiv \rho u_*^2 = \rho C_d U_{10}^2, \quad (1)$$

where ρ is the density of air, u_* is the friction velocity, and U_{10} is the wind speed at 10 m height above mean sea level. Although early works determined the drag coefficient as a constant, recent studies obtained different linear relationships between drag coefficient and wind speed from field and laboratory observations [e.g., Garratt, 1977; Large and Pond, 1981; Wu, 1980; Geernaert et al., 1986; Yelland and Taylor, 1996]. Among them the relationships of Wu [1980] and Large and Pond [1981] were widely used in estimating the air-sea momentum flux, as well as in many atmospheric, oceanic and surface wave models. However, the dependence of drag coefficient on wind speed determined by different researchers varies significantly, indicating that the drag coefficient might depend on not only the wind speed, but also other factors such as the wave development parameters like wave age and wave steepness [e.g., Geernaert et al., 1987; Guan and Xie, 2004].

[4] The other method to parameterize wind stress is through sea surface aerodynamic roughness z_0 , which is extended from the roughness in logarithmic wind profile theory over land. This method is equivalent to the bulk aerodynamic relation, equation (1), since the drag coefficient has a one-to-one correspondence with the aerodynamic roughness for neutral stratification through

$$C_d = \kappa^2 \left[\ln \left(\frac{10}{z_0} \right) \right]^{-2}, \quad (2)$$

where the reference height is 10 m, and $\kappa = 0.4$ is the von Karman constant. The sea surface roughness is widely used in numerical models to estimate sea surface wind stress.

¹Physical Oceanography Laboratory, Ocean University of China, Qingdao, China.

²Department of Marine, Earth and Atmospheric Sciences, North Carolina State University, Raleigh, North Carolina, USA.

Corresponding author: C. Guan, Physical Oceanography Laboratory, Ocean University of China, 238 Songling Rd., Qingdao, Shandong 266100, China. (clguan@ouc.edu.cn)

Table 1. Values for Charnock Constant From Different Researchers Based On Various Laboratory and Field Observations

Authors	Charnock Constant
Charnock [1958]	0.012
Kitaigorodskii and Volkov [1965]	0.035
Smith and Banke [1975]	0.0130
Garratt [1977]	0.0144
Wu [1980]	0.0185
Geernaert et al. [1986]	0.0192

Considering the dependence of sea surface roughness on wind speed and using dimensional analysis, Charnock [1955] presented the famous Charnock relation

$$gz_0/u_*^2 = \alpha, \quad (3)$$

where g is the acceleration of gravity, and α is the Charnock parameter or nondimensional roughness length, which is taken as a constant. Thereafter, various values for the Charnock constant were determined by different researchers based on different observational data (Table 1). It should be noted that a constant Charnock parameter corresponds to a linear dependence of drag coefficient on wind speed [Guan and Xie, 2004]. As mentioned above, the existence of surface waves under different wave developments could affect both the air and water side current structure, which in turn would affect the air-sea momentum flux. Measurements have also indicated that sea surface roughness depends not only on wind speed, but also on wave development. Kitaigorodskii and Volkov [1965] explicitly included the wavefield effects by using a weighted integral of the sea surface spectrum to estimate the aerodynamic roughness. Based on the similarity of wind wave spectrum, Stewart [1974] proposed an extended Charnock relation, in which the Charnock parameter α was considered as a function of wave age β_*

$$\alpha = f(\beta_*), \quad (4)$$

where β_* is defined as c_p/u_* , in which c_p is the phase speed of the spectral peak. Masuda and Kusaba [1987] further gave an exponential relationship between the Charnock parameter and the wave age

$$\alpha = n\beta_*^m, \quad (5)$$

where n and m are parameters determined by observations. When $m = 0$ and $n = \alpha$, equation (5) leads to the classical Charnock relation. However, positive (negative) m indicates the Charnock parameter increases (decreases) with the wave age. Various values of n and m were determined by different researchers based on field and laboratory observations [Jones and Toba, 2001]. Concerning the relationship between the Charnock parameter and the wave age, there are mainly two different, even opposite, kinds of viewpoints. One viewpoint believes that the nondimensional sea surface roughness decreases with the increasing wave age [Donelan, 1990; Johnson et al., 1998; Drennan et al., 2003], corresponding to negative m in equation (5). The other viewpoint considers that the nondimensional sea surface roughness increases with the increasing wave age [Toba et al., 1990; Sugimori et al., 2000], corresponding to positive m in equation (5).

However, neither of the viewpoints can explain both field and laboratory observational data well. The SCOR (Scientific Committee on Oceanic Research) workgroup 101 [Jones and Toba, 2001] proposed a relation between the Charnock parameter and wave age (SCOR relation), which shows that the nondimensional sea surface roughness first increases and then decreases with the increasing wave age. This relation can be thought of as a combination of the above mentioned two kinds of viewpoints, and it agrees well with the field and laboratory observational data.

[5] The above reviewed studies are mostly only applicable to low-to-moderate wind conditions, since they are obtained from measurements usually under wind speed smaller than 25 m s^{-1} . As for wind stress under high winds, due to lack of observation it is generally assumed that the linear relationship between drag coefficient and wind speed can be applied to high wind conditions ($>25 \text{ m s}^{-1}$) through extrapolation [Garratt, 1977; Wu, 1982]. However, recent field and laboratory observations [Alamaro, 2001; Alamaro et al., 2002; Powell et al., 2003; Donelan et al., 2004; Black et al., 2007; Jarosz et al., 2007] show that it is not suitable to simply apply the linear relation between drag coefficient and wind speed to high wind conditions. According to the existing field and laboratory observations, the drag coefficient does not increase, but decreases with the increasing wind speed under high wind conditions. It is speculated that the sea foams and sea sprays generated by wave breaking and wind tearing the breaking wave crests prevent the underneath sea surface from being dragged by the wind [Powell et al., 2003]. Under high wind conditions breaking waves disrupt the air-sea interface into a transition layer from bubble-filled water to spray-filled air, modifying the logarithmic wind profile, which in turn would affect the air-sea momentum, heat fluxes as well as mass transfer. Based on the solution of the TKE balance equation in the sea spray suspension layer and field measurements of Powell et al. [2003], Makin [2005] derived a resistance law of the sea surface at hurricane winds, predicting the reduction of the drag coefficient for the wind speed exceeding hurricane force, which is in agreement with field observational data.

[6] Although the SCOR relation can to some extent explain the field and lab observations under low-to-moderate winds, its application to high wind conditions is not supported by recent observations. It is believed that the relationship given by Makin [2005] included the effect of sea spray on wind stress under high winds, however, it did not take the wave state into account by taking the Charnock parameter as a constant. Currently, there is no parameterization for wind stress which considers both wave state and sea spray effects and is applicable to both low-to-moderate and high wind conditions. This study thus aims to propose a parameterization for wind stress applicable from low to extreme wind conditions, with both wave state and sea spray effects being taken into consideration.

2. Wave State and Sea Spray Related Parameterization of Wind Stress

2.1. Wave State Affected Wind Stress Under Low-to-Moderate Winds

[7] It has been commonly recognized that wave state has an important impact on the wind stress [Toba et al., 1990;

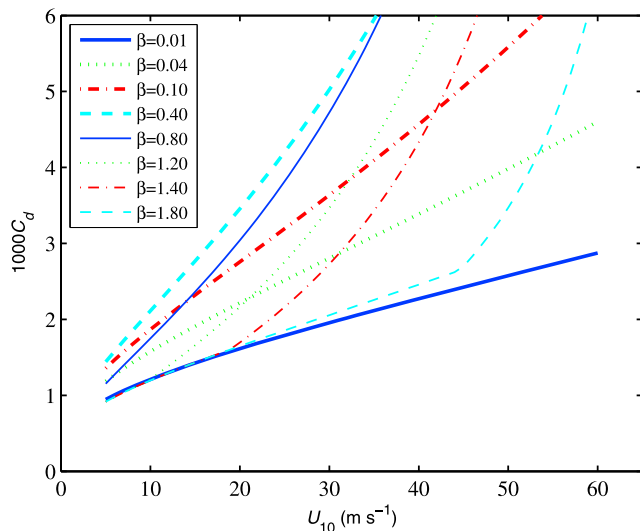


Figure 1. The relation between drag coefficient and wind speed under different wave age (β) conditions, according to the SCOR relation.

Donelan, 1990; Johnson *et al.*, 1998; Drennan *et al.*, 2003], although as reviewed above we have a debate regarding in which way the wave state would impact the wind stress. By analyzing and synthesizing a large number of field and laboratory observations, SCOR workgroup 101 [Jones and Toba, 2001] presented a relationship between the Charnock parameter α and the wave age β_* (the SCOR relation)

$$\frac{gz_0}{u_*^2} = \begin{cases} 0.03\beta_* \exp(-0.14\beta_*), & \sim 0.35 < \beta_* < 35 \\ 0.008, & \beta_* \geq 35 \end{cases} \quad (6)$$

[8] According to equation (6), the nondimensional sea surface roughness first increases and then decreases with the increasing wave age. The SCOR relation could be considered as a combination of the above mentioned two kinds of viewpoints. It agrees well with current field and laboratory observations [see Jones and Toba, 2001, Figures 10.5 and 10.6].

[9] According to the SCOR relation and using equations (1) and (2), for given wind speeds U_{10} and wave ages β defined as c_p/U_{10} , the corresponding drag coefficients can be calculated through iteration. Figure 1 shows the corresponding relation between the drag coefficient and the wind speed under different wave ages (β), from which one can see the drag coefficient increases with the wind at a given wave age β . We can also find that when the wave age β is less than about 0.4, the drag coefficient increases faster with the increasing wind speed as the wave age increases. This corresponds to that the nondimensional sea surface roughness increases with the wave age. When the wave age β is larger than about 0.4, the increasing rate of drag coefficient with wind speed will be reduced as the wave age increases. Correspondingly, under this circumstance the nondimensional sea surface roughness decreases with the increasing wave age.

[10] It should be noted that, since the SCOR relation is determined mainly from observations under low-to-moderate

wind conditions, without the consideration of other factors such as sea sprays, it is not appropriate to apply this relation to high wind conditions.

2.2. Sea Spray Affected Wind Stress Under High Winds

[11] As for the air-sea momentum flux under high wind conditions, recent observations have indicated that the wind stress levels off as the wind speed exceeds hurricane force, and instead of increasing the drag coefficient decreases with the wind speed. Through measurements in a circular wind-wave tank, Alamaro [2001] and Alamaro *et al.* [2002] found that when the wind speed exceeds about 25 m s^{-1} , the drag coefficient decreases, rather than increasing with increasing winds. Powell *et al.* [2003] analyzed lots of wind profiles measured by Global Positioning System dropwindsonde (GPS sonde) in tropical cyclones, showing that the surface momentum flux levels off as the wind speed increases above hurricane force, and the drag coefficient decrease with the increasing wind when the wind speed is larger than 33 m s^{-1} . Based on laboratory measurements, Donelan *et al.* [2004] concluded that the aerodynamic roughness approaches a limited value under high wind conditions ($>33 \text{ m s}^{-1}$). In addition, Jarosz *et al.* [2007] also concluded that for winds between 20 and 48 m s^{-1} , drag coefficient initially increases and peaks at winds of about 32 m s^{-1} before decreasing under hurricane wind conditions through the bottom-up determination of air-sea momentum exchange. According to these existing field and laboratory observations, there are two obvious characteristics for wind stress under high wind conditions: (1) The drag coefficient doesn't increase, but decreases with the increasing wind speed under high wind conditions; (2) The drag coefficient reaches its maximum when the wind speed lies in the range of 25 – 33 m s^{-1} .

[12] These characteristics of drag coefficient under high wind conditions may be due to the existence of sea foams and sea sprays.

[13] It is believed that at very high wind speeds a deep part of the marine atmospheric surface layer is filled with spray droplets, originating from intensively breaking waves, which form the spray droplet suspension layer. Makin [2005] assumed that a thin region adjacent to the sea surface part of the suspension layer is characterized by a regime of limiting saturation. Based on the solution of the TKE balance equation for the airflow in the regime of limited saturation by suspended sea spray droplets, the profile of the wind velocity is given by [Barenblatt, 1979]

$$u(z) = \left(\frac{u_*}{\kappa\omega} \right) \ln \frac{z}{z_0}, \quad (7)$$

where $u(z)$ is the wind speed at height z , z_0' the local roughness, ω is positive and satisfies the condition that $\omega = a/\kappa u_* < 1$, a is the terminal fall velocity of the droplets. It is noted that ω is the correction parameter indicating the impact of sea spray on the logarithmic wind profile. On the basis of that the separation of the airflow from short steep breaking waves at high wind speeds is responsible for the formation of the surface stress and is well described by the Charnock relation, shown by Kudryavtsev and Makin [2001], Makin [2005] assumed that the local roughness length still could

be described by the Charnock relation (3) in the regime of limiting saturation.

[14] As revealed by *Powell et al.* [2003], above the suspension layer, the wind speed could still be described by the logarithmic profile

$$u(z) = \left(\frac{u_*}{\kappa}\right) \ln \frac{z}{z_0}, \quad (8)$$

where z_0 should be interpreted as the effective roughness. It is noted that, inside the suspension layer in the regime of limiting saturation, the wind profile (7) is characterized by the slope $u_*/\kappa\omega$ and local roughness z'_0 , while above the suspension layer the wind profile is described by the logarithmic form (8) with slope u_*/κ and the effective roughness z_0 . As pointed out by *Makin* [2005], the effective roughness reflects the impact of both waves and sea spray droplets on the flow dynamics and cannot be described by the Charnock relation.

[15] By overlapping the profiles (7) and (8) at the height of the spray droplet suspension layer h_l , namely $z = h_l$, *Makin* [2005] derived a resistance law of the sea surface at hurricane winds. It can be rewritten as

$$\frac{gz_0}{u_*^2} = c_l^{1-1/\omega} \alpha^{1/\omega}, \quad (9)$$

where

$$c_l = \frac{gh_l}{u_*^2}, \quad (10)$$

$$\omega = \min(1, a_{cr}/\kappa u_*). \quad (11)$$

Here α is the Charnock constant, which is taken as 0.01 in *Makin* [2005]; c_l is the nondimensional height of sea spray droplet suspension layer. Assuming the height of the spray droplet suspension layer h_l is about 1/10 of the fully developed significant wave height H_s , *Makin* [2005] chose $c_l = 10$. Using the observational data from *Powell et al.* [2003], the critical terminal fall velocity of spray droplets a_{cr} is estimated as 0.64 m s^{-1} [*Makin*, 2005]. It is important to note that, as the wind speed is in low wind conditions with $\omega = 1$, the sea spray effect on the logarithmic wind profile and air-sea momentum flux can be neglected, the wind profile (7) tends to the logarithmic wind profile (8), and equation (9) reduces to the classic Charnock relation. Under high wind conditions smaller ω corresponds to larger impact of sea spray on the sea surface roughness, leading to the decrease of the drag coefficient and the leveling off of the wind stress. Thus, this relation can predict the reduction of the drag coefficient for the wind speed exceeding hurricane force, which agrees well with *Powell et al.*'s [2003] measurements under high winds [see *Makin*, 2005, Figure 1]. However, it should be mentioned that this relation does not explicitly consider the wave state effects on air-sea momentum flux, by taking the Charnock parameter α as a constant.

2.3. Wave State and Sea Spray Affected Wind Stress

[16] As for the wind stress under both low-to-moderate winds and high winds, by using the Charnock parameter predicted by the SCOR relation instead of the Charnock

constant, we combine the SCOR relation and the resistance law of *Makin* [2005] to obtain the following relationship:

$$\frac{gz_0}{u_*^2} = \begin{cases} c_l^{1-1/\omega} [0.03\beta_* \exp(-0.14\beta_*)]^{1/\omega}, & \sim 0.35 < \beta_* < 35 \\ c_l^{1-1/\omega} (0.008)^{1/\omega}, & \beta_* \geq 35 \end{cases}. \quad (12)$$

[17] Assuming the height of the sea spray suspension layer h_l is 1/10 of the significant wave height H_s [*Makin*, 2005], we take

$$c_l = \frac{1}{10} \frac{gH_s}{u_*^2}. \quad (13)$$

[18] Instead of using the empirical relation for the significant wave height for fully developed wind sea, we here introduce *Toba's* [1972] 3/2 power law applicable to all wind seas

$$H_* = BT_*^{3/2}, \quad B = 0.062, \quad (14)$$

where $H_* = gH_s/u_*^2$ and $T_* = gT_s/u_*$ are nondimensional significant wave height and period, respectively. Substituting equation (14) into equation (13), one can get

$$c_l = 0.0062 \left(\frac{gT_s}{u_*}\right)^{3/2}. \quad (15)$$

[19] Further using the relation between significant wave period T_s and peak wave period T_p [*Wen et al.*, 1989; *Goda and Nagai*, 1974]

$$T_s = 0.91T_p \quad (16)$$

and recalling the relation $c_p = gT_p/2\pi$ and the definition of wave age β_* , one can then obtain a wave-age-dependent nondimensional height for sea spray suspension layer

$$c_l = \begin{cases} 0.085\beta_*^{3/2}, & \sim 0.35 < \beta_* < 35 \\ 17.60, & \beta_* \geq 35 \end{cases}. \quad (17)$$

[20] Here, for fully developed conditions ($\beta_* \geq 35$) we fixed the nondimensional suspension layer height c_l at 17.60, which is the value when the wave age β_* equals to 35. One can see that as the surface wave develops the nondimensional sea spray suspension layer height c_l increases with the increasing wave age β_* . Substituting equation (17) into equation (12), a new parameterization of sea surface aerodynamic roughness is obtained as

$$\alpha = \frac{gz_0}{u_*^2} = \begin{cases} (0.085\beta_*^{3/2})^{1-1/\omega} [0.03\beta_* \exp(-0.14\beta_*)]^{1/\omega}, & \sim 0.35 < \beta_* < 35 \\ 17.60^{1-1/\omega} (0.008)^{1/\omega}, & \beta_* \geq 35 \end{cases}, \quad (18)$$

where z_0 is aerodynamic roughness, β_* is wave age, and ω is correction parameter indicating the impact of sea spray on

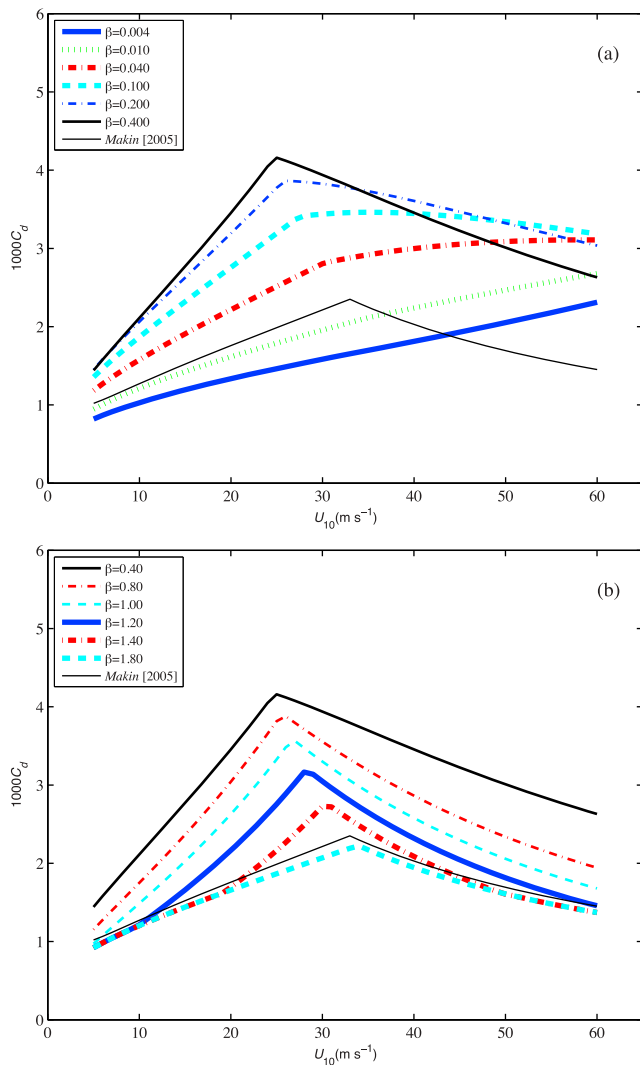


Figure 2. The relation between drag coefficient and wind speed under different wave age (β) conditions, corresponding to the wave age and sea spray related parameterization: (a) for wave ages (β) less than about 0.4 and (b) for wave ages (β) larger than about 0.4. The relation of *Makin* [2005] is also included for comparison.

the logarithmic wind profile, which can be estimated through equation (11) with $a_{cr} = 0.64 \text{ m s}^{-1}$ [*Makin*, 2005]. With the effects of both wave state and sea spray on air-sea momentum flux, the new proposed parameterization is applicable from low-to-moderate wind conditions to extreme wind conditions. From equation (18), under low-to-moderate wind conditions when the sea spray effects are negligible ($\omega = 1$), this parameterization reduces to the SCOR relation with the Charnock parameter first increasing and then decreasing as the wave age increases. Under high wind conditions when sea sprays begin to have significant effects ($\omega < 1$), the sea surface roughness and drag coefficient decrease with the increasing wind speed.

[21] According to the new proposed parameterization and by using equations (1) and (2), for given wind speeds U_{10} and wave ages β , the corresponding drag coefficients can be calculated through iteration. Figure 2 shows the

corresponding relation between drag coefficient and wind speed under different wave developments, with (a) for wave age β less than 0.4 and (b) for wave age β greater than 0.4. From both Figures 2a and 2b, one can find that under high winds the drag coefficient decreases with increasing wind speed. This is in agreement with the above mentioned first characteristic of the existing measurements under high wind conditions. Sea sprays generated by wave breaking and wind tearing wave crests modify the wind profile and prevent the water surface from being dragged by the wind directly, which in turn, reduces the drag coefficient and levels off the wind stress under high winds. Besides, the acceleration from relatively slow-moving water surface to airflow of the sea spray droplets which evaporate or suspend in the air may also play a role in reducing the sea surface drag coefficient. It is also shown in Figure 2b that the relation of *Makin* [2005] is very close to the curve corresponding to wave age of 1.8. As for the wave state effects especially under low-to-moderate winds, for wave age smaller than 0.4, younger waves usually correspond to smaller drag coefficients Figure 2a; whereas for wave age larger than 0.4, mature waves correspond to smaller drag coefficients Figure 2b. This wave age dependence is consistent with the SCOR relation [*Jones and Toba*, 2001]. However, under high wind conditions, the interaction between wave state effects and sea spray effects makes the dependence of drag coefficient on wind speed more complicated. Generally, with younger waves, one would expect less sea sprays generated from wave breaking, thus less impact from sea sprays on the drag coefficient; whereas with larger wave ages, the impact of sea sprays becomes more obvious Figure 2. Comparing Figure 2a to Figure 1, one can see that, for very small wave ages (e.g., $< \sim 0.01$), sea spray effects on drag coefficient are hardly seen for wind speed up to 60 m s^{-1} . There is also a limiting case here. In the case of wave age $\beta \rightarrow 0$, i.e., without surface waves, the drag coefficient as well as the sea surface roughness tends to be constant, which is similar to those under wall boundary conditions. From Figure 2 one can also find that, the drag coefficients corresponding to different wave states reach their maximum values when the wind speeds lie in the range of $25\text{--}33 \text{ m s}^{-1}$, which agrees well with the above mentioned second characteristic of the existing measurements under high wind conditions. This means that the sea spray takes effect as the wind speed approaches the range of $25\text{--}33 \text{ m s}^{-1}$. In fact, this feature is fairly consistent with the argument by *Amorocho and DeVries* [1980] that a state of breaker saturation is reached in the neighborhood of wind speed of 20 m s^{-1} . At these wind speed ranges, sea surface wind begins to drag sea sprays and sea foams rather than dragging the true sea surface waves directly. As the wave age increases from about 0.04 to 0.4, the wind speeds at which the drag coefficients begin to level off or decrease for different wave ages gradually decrease to about 25 m s^{-1} ; while as the wave age increases from about 0.4, the wind speed wind speeds at which the drag coefficients begin to decrease for different wave ages gradually increases from about 25 to 33 m s^{-1} . It can also be noticed that, under most wave ages (larger than 0.1) the larger the drag coefficient, the lower wind speed at which the drag coefficient begin to decrease or level off.

[22] Correspondingly, the relation between friction velocity and wind speed and the relation between sea surface

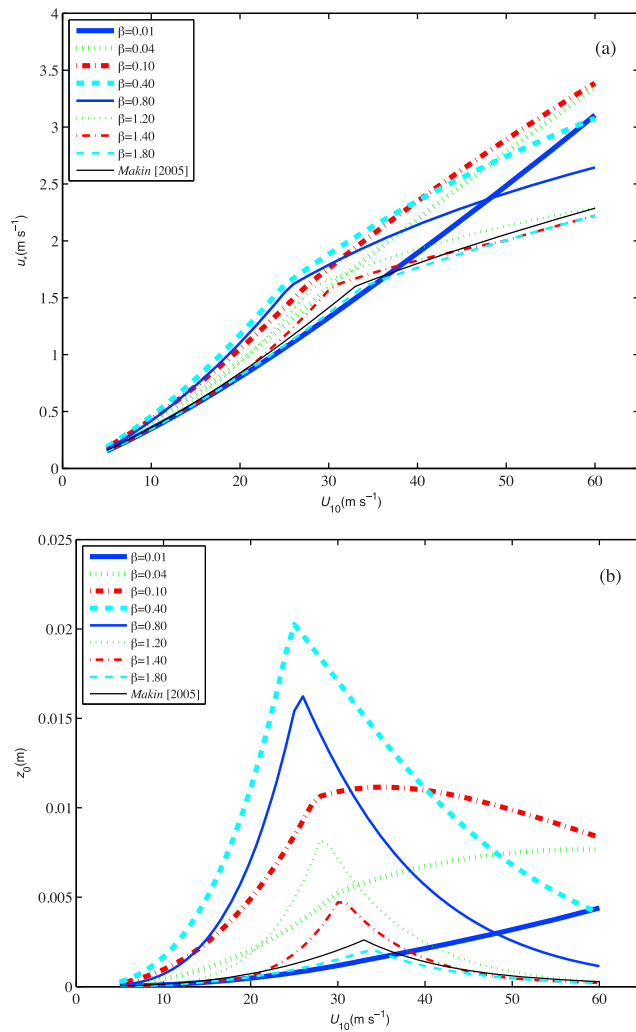


Figure 3. The relations (a) between friction velocity and wind speed and (b) between sea surface roughness and wind speed, under different wave age (β) conditions, according to the wave age and sea spray related parameterization. The relations from Makin [2005] are also included for comparison.

effective roughness and wind speed under different wave age (β) conditions are given in Figure 3. One can see that under all wave age conditions, the friction velocity (u_*) increases with surface wind continuously. This is because surface wind speed is the major factor for air-sea momentum flux even though the drag coefficient reaches its maximum value at the wind speed range of 25 to 33 m s^{-1} . The reduction of drag coefficient under high wind conditions only reduces the increasing rate of the friction velocity (wind stress) over wind speed. As for the sea surface roughness (z_0), under different wave age conditions, it first increases with increasing surface winds and then decreases or levels off with increasing surface winds. Also, for wave ages less than 0.4, sea surface roughness increases with increasing wave ages, whereas for wave ages greater than 0.4, sea surface roughness decreases with increasing wave ages. For all wave development conditions, sea surface roughness has its maximum value of around 0.02 m (corresponding to the

maximum drag coefficient of value of about 0.0042) at wave age (β) of 0.4 and wind speed of 25 m s^{-1} or so.

3. Validation and Discussion

[23] As mentioned above, the proposed relationship would be the same as the SCOR relation under low-to-moderate wind conditions when sea spray effects are negligible. Detailed validation for the SCOR relation and its comparison against various field and laboratory observations can be found in Jones and Toba [2001]. In this study, we will mainly focus on the behavior of the new proposed relationship under high wind conditions. Some recent field [Powell et al., 2003; Powell, 2006; Jarosz et al., 2007] and laboratory [Alamaro, 2001; Donelan et al., 2004] data sets with observations under high winds described below are used to be compared with the new relationship.

3.1. Field and Laboratory Observational Data Sets Under High Winds

[24] In a circular wind-wave tank made of two concentric walls (with the outer and inner radii being 0.479 and 0.284 m, respectively), Alamaro [2001] measured the water velocity by an Acoustic Doppler Velocimeter (ADV) and the air velocity by an anemometer. A paddle powered by an electric motor can move the air over the water surface at high wind speeds. Through the “spin-down” experiments which provide information on the deceleration of the water mass, the shear stress over the water surface owing to the airflow and thus the drag coefficient can then be calculated under different measured air velocities. The tank was equipped with an adjustable false bottom, enabling the use of different distances from the paddle to the water surface for the same water depth. Also, the water depth can be varied in the tank. Nine sets of experiments with different water depths of 10, 12, and 14 cm and different false bottom depths ranging from 0 to 15 cm were conducted. The measurements show that the drag coefficient begins to decrease with increasing winds when wind speed is larger than about 25 m s^{-1} .

[25] Powell et al. [2003] analyzed 331 of wind profiles measured by GPS dropsonde in the vicinity of the hurricane eye walls during 1997–1999. Wind profiles were organized into different groups based on the mean boundary layer (MBL) wind speed. Drag coefficient and surface roughness were then estimated through the profile method by using the wind profiles between different layers: 10–100 m, 10–150 m, 20–100 m, and 20–150 m, for each MBL group. The results show that the sea surface stress levels off as the wind speeds increase above hurricane force, and the drag coefficient decrease with increasing wind when wind speed is larger than 33 m s^{-1} . With the GPS dropsonde profiles being updated to include measurements till 2005, Powell [2006] found that the drag coefficient increases with wind up to 41 m s^{-1} and then decrease with increasing wind based on 1270 GPS dropsonde profiles for several MBL wind speed groups. He also analyzed the azimuthal dependence of the drag coefficient for hurricanes. As in Black et al. [2007], a storm can be divided into three regions: (1) rear sector (151° – 240° relative to the storm motion vector) with waves moving with the wind, (2) right sector (21° – 150°) with waves moving outward by up to 45° relative to the wind, and (3) left front sector (241° – 20°) where waves travel outward at 60° – 90° to the wind. The

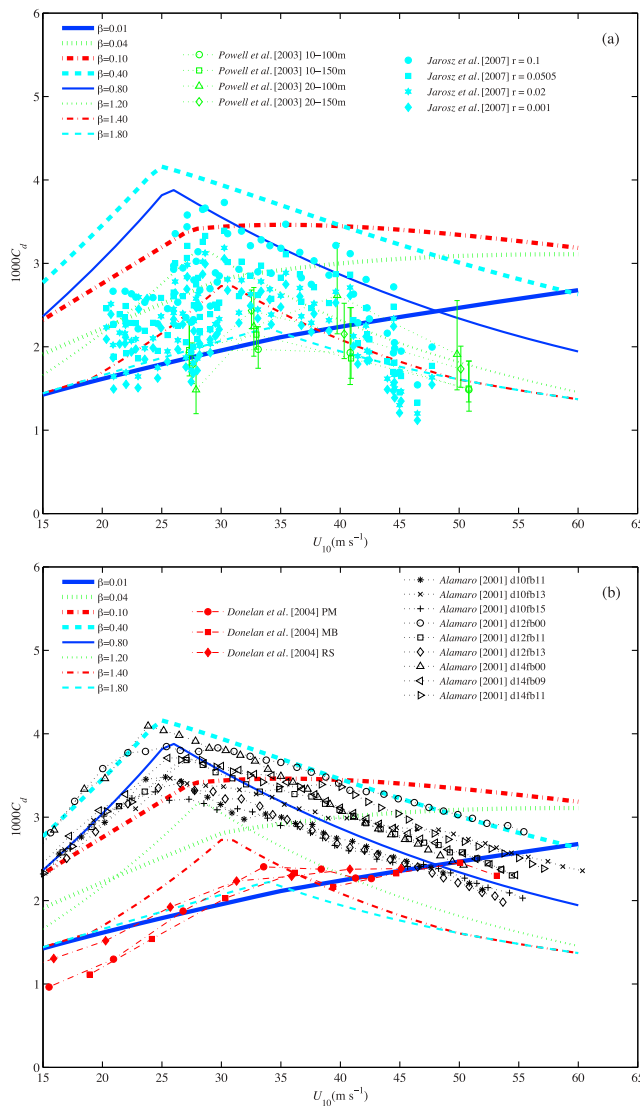


Figure 4. Comparison between the drag coefficient and wind speed relations under different wave ages (color lines), corresponding to the wave age and sea spray related parameterization and (a) various field and (b) laboratory observations under high winds. The green markers with error bars and dotted lines are field measurements from Powell *et al.* [2003]. The cyan markers are the field measurements from Jarosz *et al.* [2007] based on different resistance coefficients ($r = 0.001, 0.02, 0.0505, \text{ and } 0.1 \text{ cm s}^{-1}$). The black markers with dotted lines are the laboratory measurements for different water depths ($d = 10, 12, \text{ and } 14 \text{ cm}$) and different false bottoms (fb, ranging from 0 to 15 cm) from Alamaro [2001]. The red markers with dash-dotted lines are laboratory measurements from Donelan *et al.* [2004] through different methods (PM, profile method; MB, momentum budget method; RS, Reynolds stress method). In general, waves measured in laboratory experiments (e.g., Alamaro's [2001] and Donelan *et al.*'s [2004] data) are younger than those measured in field experiments (e.g., Powell *et al.*'s [2003] and Jarosz *et al.*'s [2007] data). And waves in a circular tank (Alamaro's [2001] data) tend to have larger wave ages than in a regular wave tank (Donelan *et al.*'s [2004] data).

results show that the drag coefficient in the left front sector is most sensitive to wind speed and is higher than those in the right and rear sectors for most wind speeds. Also, the drag coefficient in the rear sector is slightly higher than in the right sector for winds up to 35 m s^{-1} , but the two sectors are similar for winds up to 42 m s^{-1} . As wave states in these sectors are usually different from each other, these results may indicate dependence of the drag coefficient on wave development.

[26] Donelan *et al.* [2004] utilized the Air-Sea Interaction Facility at the University of Miami to examine the wind stress under high winds. The facility includes a tank which is 15 m long in its working section and 1 m wide with its height of 1 m divided equally between air and water. It can generate winds along the centerline in the range of 0 to 30 m s^{-1} . The wind was measured at 0.3 m height and was extrapolated to the standard meteorological height of 10 m using the logarithmic wind profile. Three methods including profile, eddy correlation, and momentum budget of water control volume, were used to estimate wind stress and thus drag coefficient under different winds. Their laboratory measurements show a saturation of the drag coefficient once the wind speed exceeds 33 m s^{-1} .

[27] Jarosz *et al.* [2007] used the bottom-up determination method of air-sea momentum exchange based on oceanside current observations to estimate sea surface wind stress under hurricane wind conditions. Their analyses were based on the observations by six current and wave/tide gauge moorings on the outer continental shelf in the northeastern Gulf of Mexico as Hurricane Ivan passed directly over them on 15 September 2004. Assuming that the directly forced ocean response on the continental shelf could be well described to the first order by the linear time-dependent depth-integrated horizontal momentum equations (especially for the along-shelf momentum), the drag coefficient can be estimated by the along-shelf momentum balance with the full water column current measurements for a given the resistance coefficient (r) at the seafloor. For four different values of the resistance coefficient: 0.001, 0.02, 0.0505, and 0.1 cm s^{-1} , Jarosz *et al.* [2007] obtained four sets of drag coefficients under wind speeds ranging from 20 to 48 m s^{-1} . Their results also found that the drag coefficient initially increases and peaks at winds of about 32 m s^{-1} before decreasing.

3.2. Comparison Between the Proposed Parameterization and Observational Data

[28] Figure 4 shows the comparison of the relation between drag coefficient and wind speed for the new presented wave state and sea spray related parameterization with the field and laboratory observational data. Since we are mainly concerned with the high wind conditions here, only the observational data with wind speed greater than 15 m s^{-1} are shown in the figure. From Figure 4, one can see that the new presented relation can cover the range of the existing field and laboratory observations well, and can explain the scatter of current measurements to some extent. The reduction of the drag coefficient under high wind conditions is shown in both the observations and the presented relation for different wave states. The drag coefficients reach their maximum values in the wind speed range of $25\text{--}33 \text{ m s}^{-1}$. The largest maximum value ($\sim 4.2 \times 10^{-3}$) based on the presented relation is very

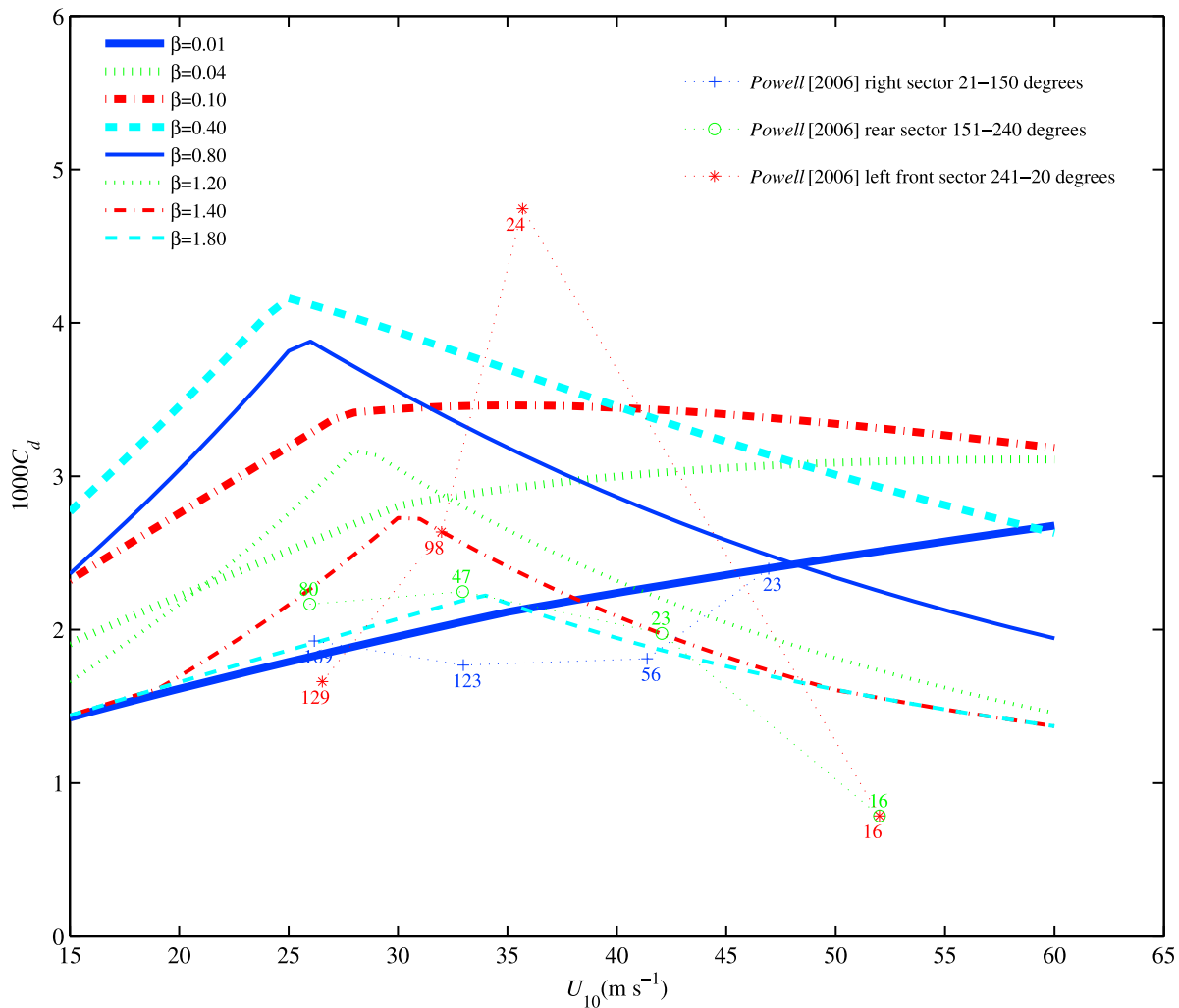


Figure 5. The relation between drag coefficient and wind speed under different wave ages (β), corresponding to the wave age and sea spray related parameterization, together with the observations from Powell [2006] for different sectors: right (21° – 150°), rear (151° – 240°), and left front (241° – 20°) of hurricanes.

close to those in Alamaro's [2001] laboratory measurements and in Jarosz *et al.*'s [2007] field measurements with the resistance coefficient of 0.1 cm s^{-1} . Also, Powell [2006] reported that the drag coefficient values can be up to 4.7×10^{-3} in the front left sector of the storm (see his Figure 15), when analyzing the azimuthal dependence of the drag coefficient around tropical cyclones. In addition, it can also be seen in the observational data that the larger the drag coefficient, the lower wind speed at which the drag coefficient begins to decrease tends to be. For both the field and laboratory data, the drag coefficients at a specific wind speed are rather scattered. A possible reason could be that those data were measured under different wave states. For example, waves in laboratory are usually younger than those in field observations. And waves in a circular tank [e.g., Alamaro, 2001] tend to have larger wave ages than waves in a regular wave tank [e.g., Donelan *et al.*, 2004] with 15 m long working section. According to the presented relation in this study, the drag coefficients with moderate wave ages (e.g., Alamaro's [2001] data) tend to be larger than those with smaller wave ages (e.g., Donelan *et al.*'s [2004] data) and

larger wave ages (e.g., Powell *et al.*'s [2003] data). This is consistent with the behavior of the observational data shown in Figure 4.

[29] In order to partly demonstrate the wave state impacts on wind stress and drag coefficient, Figure 5 shows the comparison of the relation between drag coefficient and wind speed for the new presented wave state and sea spray related parameterization with the observational data for different sectors of tropical cyclones from Powell [2006] when analyzing the azimuthal dependence of the drag coefficient for hurricanes. The blue, green, and red markers with dotted lines correspond to observations in the right (21° – 150°), rear (151° – 240°), and left front (241° – 20°) sectors, respectively. The drag coefficients in the left front sector are larger than those in the rear and right front. As is known, waves are usually very young in the rear sector, moderate in the left and front sector, while older in the right sector. This wave age distribution around a tropical cyclone can also be seen in Moon *et al.* [2004, Figures 9c and 9d]. From Figure 5, one can see that, for wind speeds in the range of 25 to 42 m s^{-1} the left front sector, usually with moderate wave ages, has

the largest drag coefficient. This is also consistent with the behavior of the wave state and sea spray related parameterization presented in this study.

[30] Although the above comparisons demonstrate some wave age impacts on the drag coefficients qualitatively, it should be pointed out that simultaneously measured air-sea momentum flux, wind and wave conditions under both low-to-moderate and especially under high wind conditions are needed in order to fully validate the presented wave state and sea spray related wind stress parameterization. Those simultaneous observations are, however, very rare especially under high winds. Thus, further field and laboratory experiments measuring wind and wave data simultaneously especially under high winds are needed to investigate the behavior of air-sea momentum flux under high wind conditions.

4. Concluding Remarks

[31] Coupling of the atmosphere to the ocean through sea surface wave processes is particularly important and impacts numerous scientific and engineering air-sea disciplines [Sullivan and McWilliams, 2010]. Parameterization of air-sea momentum flux, which is one of the fundamental processes that connect atmosphere, waves and ocean, under various wind conditions is critical to both small-scale and large-scale air-sea interactions as well as the coupling among the atmosphere-wave-ocean system. In this study, a sea surface aerodynamic roughness parameterization applicable from low to extreme winds is proposed by considering the effects of wave state and sea spray on air-sea momentum flux. According to the new presented parameterization, under low wind conditions when the effect of sea spray could be neglected, the nondimensional sea surface roughness first increases and then decreases with the increasing wave age, which is consistent with the SCOR relation [Jones and Toba, 2001]. While under high wind conditions, the drag coefficient does not increase, but decreases with the increasing wind speed due to the effect of sea spray, and this agrees well with recent observations under high winds. In addition, the drag coefficients under different wave ages reach their maximum values when wind speeds are in the range of 25–33 m s⁻¹, which is also supported by recent field and laboratory measurements. Correspondingly, the sea surface aerodynamic roughnesses reach their maximum values with wind speeds in the range of 25–33 m s⁻¹ for different wave developments. The reduction of drag coefficient under high winds thus slows down the increasing rate of friction velocity with increasing wind speed.

[32] As the wave state and sea spray would affect the air-sea momentum flux as well as air-sea heat and mass fluxes, the new presented parameterization could be used in coupled atmosphere-wave-ocean modeling systems, which in turn could be used to investigate the effects of air-sea interaction on coupled air-sea systems. Furthermore, as the current presented parameterization of wind stress includes the sea spray effects and is applicable to extreme wind conditions, it could also be used in the simulations of tropical cyclone systems such as hurricanes and typhoons.

[33] However, it should be noted that the new proposed parameterization needs to be further validated through simultaneously measured wind and wave data especially under high wind conditions. More field and laboratory

experiments should also be conducted to investigate the dependence of wind stress on other factors such as atmospheric stratification, surface tension, wind gust, rain, and so on.

[34] **Acknowledgments.** The authors are grateful for the English proofreading by Katie Costa. The efforts of the researchers who obtained and published the data sets used in this study as well as their funding organizations are much appreciated. This work is supported by National Natural Science Foundation of China (40830959 and 40921004) and Ministry of Science and Technology of China (2011BAC03B01), the U.S. National Oceanic and Atmospheric Administration (NOAA) through subcontract UF-EIES1100D31-NCS, and the U.S. Southeast Coastal Ocean Observing Regional Association (SECOORA) award IOO.11(03)NCSU.LX.MOD.1.

References

- Alamaro, M. (2001), Wind wave tank for experimental investigation of momentum and enthalpy transfer from the ocean surface at high wind speed, MS thesis, 77 pp., Mass. Inst. of Technol., Cambridge.
- Alamaro, M., K. A. Emanuel, J. J. Colton, W. R. McGillis, and J. Edson (2002), Experimental investigation of air-sea transfer of momentum and enthalpy at high wind speed, paper presented at 25th Conference on Hurricanes and Tropical Meteorology, Am. Meteorol. Soc., San Diego, Calif., 29 Apr to 3 May.
- Amorcho, J., and J. J. DeVries (1980), A new evaluation of the wind stress coefficient over water surface, *J. Geophys. Res.*, *85*(C1), 433–442, doi:10.1029/JC085iC01p00433.
- Barenblatt, G. I. (1979), *Similarity, Self-Similarity, and Intermediate Asymptotics*, 218 pp., Consultants Bureau, New York.
- Black, P. G., E. A. D'Asaro, T. B. Sanford, W. M. Drennan, J. A. Zhang, J. R. French, P. P. Niiler, E. J. Terrill, and E. J. Walsh (2007), Air-sea exchange in hurricanes: Synthesis of observations from the coupled boundary layer air-sea transfer experiment, *Bull. Am. Meteorol. Soc.*, *88*(3), 357–374, doi:10.1175/BAMS-88-3-357.
- Charnock, H. (1955), Wind stress on a water surface, *Q. J. R. Meteorol. Soc.*, *81*, 639–640, doi:10.1002/qj.49708135027.
- Charnock, H. (1958), A note on empirical wind-wave formulae, *Q. J. R. Meteorol. Soc.*, *84*, 443–447, doi:10.1002/qj.49708436212.
- Donelan, M. A. (1990), Air-sea interaction, in *The Sea: Ocean Engineering Science*, edited by B. L. Mehaute and D. M. Hanes, pp. 239–292, Wiley-Interscience, New York.
- Donelan, M. A., B. K. Haus, N. Reul, W. J. Plant, M. Stiassnie, H. C. Graber, O. B. Brown, and E. S. Saltzman (2004), On the limiting aerodynamic roughness of the ocean in very strong winds, *Geophys. Res. Lett.*, *31*, L18306, doi:10.1029/2004GL019460.
- Drennan, W. M., H. C. Graber, D. Hauser, and C. Quentin (2003), On the wave age dependence of wind stress over pure wind seas, *J. Geophys. Res.*, *108*(C3), 8062, doi:10.1029/2000JC000715.
- Edson, J., et al. (2007), The coupled boundary layers and air-sea transfer experiment in low winds, *Bull. Am. Meteorol. Soc.*, *88*(3), 341–356, doi:10.1175/BAMS-88-3-341.
- Gao, Z., Q. Wang, and S. Wang (2006), An alternative approach to sea surface aerodynamic roughness, *J. Geophys. Res.*, *111*, D22108, doi:10.1029/2006JD007323.
- Garratt, J. R. (1977), Review of drag coefficients over oceans and continents, *Mon. Weather Rev.*, *105*(7), 915–929, doi:10.1175/1520-0493(1977)105<0915:RODCOO>2.0.CO;2.
- Geernaert, G. L., K. B. Katsaros, and K. Richter (1986), Variations of the drag coefficient and its dependence on sea state, *J. Geophys. Res.*, *91*, 7667–7679, doi:10.1029/JC091iC06p07667.
- Geernaert, G. L., S. E. Laresn, and F. Hansen (1987), Measurements of the wind stress, heat flux, and turbulence intensity during storm conditions over the North Sea, *J. Geophys. Res.*, *92*(C12), 13,127–13,139, doi:10.1029/JC092iC12p13127.
- Goda, Y., and K. Nagai (1974), Investigation of the statistical properties of sea waves with fields and simulated data, *PHRI Rep. 013-01-01*, Wave Lab., Mar. Hydrodyn. Div., Port and Harbour Res. Inst., Minist. of Transp., Yokosuka, Japan.
- Guan, C., and L. Xie (2004), On the linear parameterization of drag coefficient over sea surface, *J. Phys. Oceanogr.*, *34*(12), 2847–2851, doi:10.1175/JPO2664.1.
- Jarosz, E., D. A. Mitchell, D. W. Wang, and W. J. Teague (2007), Bottom-up determination of air-sea momentum exchange under a major tropical cyclone, *Science*, *315*(5819), 1707–1709, doi:10.1126/science.1136466.
- Johnson, H. K., J. Hojstrup, H. J. Vested, and S. E. Larsen (1998), On the dependence of sea surface roughness on wind waves, *J. Phys. Oceanogr.*,

- 28(9), 1702–1716, doi:10.1175/1520-0485(1998)028<1702:OTDOSS>2.0.CO;2.
- Jones, I. S. F., and Y. Toba (Eds.) (2001), *Wind Stress Over the Ocean*, 307 pp., Cambridge Univ. Press, Cambridge, U. K., doi:10.1017/CBO9780511552076.
- Kitaigorodskii, S. A., and Y. A. Volkov (1965), On the roughness parameter of the sea surface and calculation of momentum flux in the near-water layer of the atmosphere, *Izv. Russ. Acad. Sci. Atmos. Oceanic Phys.*, *1*, 973–988.
- Kudryavtsev, V. N., and V. K. Makin (2001), The impact of air-flow separation on the drag of the sea surface, *Boundary Layer Meteorol.*, *98*, 155–171, doi:10.1023/A:1018719917275.
- Lange, B., H. K. Johnson, S. Larsen, J. Hojstrup, H. Kofoed-Hansen, and M. J. Yelland (2004), On detection of a wave age dependency for the sea surface roughness, *J. Phys. Oceanogr.*, *34*(6), 1441–1458, doi:10.1175/1520-0485(2004)034<1441:ODOAWA>2.0.CO;2.
- Large, W. G., and S. Pond (1981), Open ocean momentum flux measurements in moderate to strong winds, *J. Phys. Oceanogr.*, *11*(3), 324–336, doi:10.1175/1520-0485(1981)011<0324:OOMFMI>2.0.CO;2.
- Makin, V. K. (2005), A note on the drag of the sea surface at hurricane winds, *Boundary Layer Meteorol.*, *115*, 169–176, doi:10.1007/s10546-004-3647-x.
- Masuda, A., and T. Kusaba (1987), On the local equilibrium of winds and wind-waves in relation to surface drag, *J. Oceanogr.*, *43*, 28–36.
- Moon, I. J., I. Ginis, and T. Hara (2004), Effect of surface waves on air–sea momentum exchange. Part II: Behavior of drag coefficient under tropical cyclones, *J. Atmos. Sci.*, *61*, 2334–2348, doi:10.1175/1520-0469(2004)061<2334:EOSWOA>2.0.CO;2.
- Petersen, G. N., and I. A. Renfrew (2009), Aircraft-based observations of air–sea fluxes over Denmark Strait and the Irminger Sea during high wind speed conditions, *Q. J. R. Meteorol. Soc.*, *135*(645), 2030–2045, doi:10.1002/qj.355.
- Powell, M. D. (2006), Final report to the National Oceanic and Atmospheric Administration (NOAA) Joint Hurricane Testbed (JHT) Program, final report, 26 pp., Atl. Oceanogr. and Meteorol. Lab., Miami, Fla.
- Powell, M. D., P. J. Vickery, and T. A. Reinhold (2003), Reduced drag coefficient for high wind speeds in tropical cyclones, *Nature*, *422*, 279–283, doi:10.1038/nature01481.
- Smith, S. D., and E. G. Banke (1975), Variation of the sea surface drag coefficient with wind speed, *Q. J. R. Meteorol. Soc.*, *101*, 665–673, doi:10.1002/qj.49710142920.
- Smith, S. D., et al. (1992), Sea surface wind stress and drag coefficients: The HEXOS results, *Boundary Layer Meteorol.*, *60*, 109–142, doi:10.1007/BF00122064.
- Stewart, R. W. (1974), The air–sea momentum exchange, *Boundary Layer Meteorol.*, *6*, 151–167, doi:10.1007/BF00232481.
- Sugimori, Y., M. Akiyama, and N. Suzuki (2000), Ocean measurement and climate prediction-expectation for signal processing, *J. Signal Process.*, *4*, 209–222.
- Sullivan, P. P., and J. C. McWilliams (2010), Dynamics of winds and currents coupled to surface waves, *Annu. Rev. Fluid Mech.*, *42*, 19–42, doi:10.1146/annurev-fluid-121108-145541.
- Toba, Y. (1972), Local balance in the air–sea boundary process, part I. On the growth process of wind waves, *J. Oceanogr.*, *28*, 109–120.
- Toba, Y., N. Iida, H. Kawamura, N. Ebuchi, and I. S. F. Jones (1990), The wave dependence of sea-surface wind stress, *J. Phys. Oceanogr.*, *20*, 705–721, doi:10.1175/1520-0485(1990)020<0705:WDOSSW>2.0.CO;2.
- Wen, S., D. Zhang, P. Guo, and B. Chen (1989), Parameters in wind-wave frequency spectra and their bearing on spectrum forms and growth, *Acta Oceanol. Sin.*, *8*, 15–39.
- Wu, J. (1980), Wind-stress coefficients over sea surface near neutral conditions—A revisit, *J. Phys. Oceanogr.*, *10*, 727–740, doi:10.1175/1520-0485(1980)010<0727:WSCOSS>2.0.CO;2.
- Wu, J. (1982), Wind-stress coefficients over sea surface from breeze to hurricane, *J. Geophys. Res.*, *87*, 9704–9706, doi:10.1029/JC087iC12p09704.
- Yelland, M. J., and P. K. Taylor (1996), Wind stress measurements from the open ocean, *J. Phys. Oceanogr.*, *26*, 541–558, doi:10.1175/1520-0485(1996)026<0541:WSMFTO>2.0.CO;2.